Heliyon 6 (2020) e03748

Contents lists available at ScienceDirect

Heliyon

journal homepage: www.cell.com/heliyon

Research article

Effect of size variation on microbubble mass transfer coefficient in flotation and aeration processes

Nyoman Suwartha [a,*], Destrianti Syamzida [a], Cindy Rianti Priadi [a], Setyo Sarwanto Moersidik [a], Firdaus Ali [b]

[a] Environmental Engineering Study Program, Department of Civil Engineering, Faculty of Engineering, Universitas Indonesia, Kampus UI Depok, Depok, 16424, Indonesia
[b] Indonesia Water Institute, Tanjung Barat, DKI Jakarta, 12530, Indonesia

ARTICLE INFO

Keywords:
Chemical engineering
Environmental science
Water treatment
Green engineering
Environmental chemical engineering
Water pollution
Aeration
Flotation
Mass transfer coefficient
Microbubble
Rising velocity

ABSTRACT

Microbubble technology dramatically raises the efficiency of the flotation and aeration processes of water treatment plants (WTPs), which see extensive use in developed countries. A local institution, Indonesia Water Institute, has tried to investigate microbubble technology intended for lab-scale WTP. However, the current reactor system does not yet meet the microbubble criteria, especially as it has had few investigations of its abilities in flotation and aeration. This study aims to analyze the effect of size variations that affect the rising velocity and mass transfer coefficient (kLa) of aeration contact time. Three local spargers were used to produce microbubbles. Bubble diameters were measured optically and analyzed using ImageJ software. The dissolved oxygen (DO) concentration was measured every minute using an automated sensor so that the kLa could be determined. Of the three spargers, the smallest bubble size was produced by the vortex type with an average bubble diameter of 89 μm and the slowest rising velocity of 17.67 m/h. It also yielded the highest kLa of 0.297/min, which gave an aeration contact time of 3.64 minutes. The experimental uses of three local spargers revealed that the smaller the microbubble diameter, the higher the mass transfer coefficient in flotation and aeration processes. This research can be the basis for developing microbubble technology for WTP in Indonesia.

1. Introduction

According to Food and Agriculture Organization of the United Nations (FAO) (2016), in Indonesia, raw water is obtained from 84.4% of surface water (lakes, rivers, and reservoirs) and 15.54% of groundwater (dug wells and drilled wells). Data from 2015 show, however, that of 100 rivers in 33 provinces in Indonesia, 52 were heavily polluted and 20 were moderately polluted [1]. That condition reflects pollution in water when river capacity to assimilate contaminant reach its limitation [2].This certainly burdens clean water treatment plants (WTPs) in the distribution of water to users.

Water treatment using microbubbles is an emerging technology because of its superior efficiency and quality compared to conventional methods [3, 4, 5]. Microbubble technology uses less coagulant than conventional coagulation to float the floc to the surface. Indeed, microbubble technology, as a form of physical-chemical processing, can accelerate the process of flocculation and flotation as well as high-level aeration in WTPs [6, 7, 8]. This technology is one of the WTP optimizations that improve sustainability while resolving polluted raw water problems [9]. Bubbles capture floc and bring it to the water surface, a process often referred to as "dissolved air flotation," by the mechanisms of bubble adhesion, nucleation, entrapment, and entrainment [2, 10]. Microbubbles can also enhance the speed of oxidation more than conventional aeration units due to greater mass transfer than conventional air supply [4, 11]. Thus, microbubble technology can solve the increasing demands of clean water treatment. One important component of microbubble technology is the sparger design [12, 13]. In general, two types of spargers exist: an advanced sparger called a "microbubble generator" (MBG) and a conventional sparger in the form of a gas distributor [12].

The microbubble technology has been applied by many developed countries, such as Korea, Japan, and the People's Republic of China. In Japan, MBG has been generally sold by local manufacturers, such as Aura Tech Co., Ltd, Shigen Kaihatsu Co., Ltd, and Nanoplanet Co., Ltd [12]. The developed microbubbles in other parts of the world though it is advance in technology but relatively expensive, laborious works in

* Corresponding author.
E-mail address: nsuwartha@eng.ui.ac.id (N. Suwartha).

https://doi.org/10.1016/j.heliyon.2020.e03748
Received 4 February 2020; Received in revised form 31 March 2020; Accepted 1 April 2020

transporting to developing countries, not easy to use (un-doable) directly, and spare parts may difficult to find. Moreover, microbubble technology has yet to see implementation on a large scale for water treatment in Indonesia. Most of Indonesian users have only implemented the technology in fishery processing and small-scale industrial labs [14, 15]. Thus, Indonesia has no common sparger manufacturing. This is due to the absence of in-depth research conducted in Indonesia and the relatively high expense of microbubble operation because of its combination of a water pump and air compressor [12]. Nevertheless, the efficiency of microbubble technology outweighs its energy consumption and operational cost [16]. Therefore, the idea of this research is to establish a new, simple yet economically low-cost, doable microbubble technology that can be easily used in laboratory or field scale.

The sparger plays an important role in the formation of microbubble size and determines the rising velocity of captured flocs and the time bubbles take to transfer mass into bulk liquid (oxygen) [7, 8]. Many investigations have observed the technology's level of effective transportation and mass transfer with different impacts. Authors [14] studied various types of spargers with image processing, producing bubbles with diameters smaller than 100 μm with variations in air flowrate of 0.1–0.6 L/min. However, they did not analyze the effect of each sparger on bubble characteristics, such as gas hold-up, mass transfer coefficient, and bubble quantity. Moreover, their study only focused on biological processing. Authors [10] studied the characterization of bubbles using image processing to focus on flotation and found a dominant rising velocity of 55–65 m/h and floc sizes smaller than 1.9 mm. However, no variations of sparger type were made, and no bubble size was analyzed (directly with flocs). Authors [12] analyzed sparger variations, namely, gas distributors (hollow plates, porous plates, and porous membranes) and MBG. They found the bubble characteristics, the mass transfer coefficient of oxygen, and gas hold-up with each sparger at 10000/s for kLa and greater than 0.05 mm/s for MBG spiral spargers. However, they did not present the diameters and quantities of the microbubbles from each sparger, as their research focused on biological processing. Authors [17] studied microbubble performance for flotation process in raw water clarification. Without the help of coagulant, the flotation reached 2 NTU clarity from 25 NTU raw water by the help of micro-sized bubble that caused by high efficiency separation [17]. However, they did not present the influence of mass transfer.

In Indonesia, the Indonesia Water Institute (IWI) owns a microbubble reactor designed for physical-chemical treatment for WTPs. However, the shortcomings of the MBG tool at the IWI include inconsistencies in the number and diameters of microbubbles produced, bubbles that appear uneven in micro-size, and bubbles were not evaluated in terms of size and quantity [18]. Therefore, the research literature lacks a study of the bubble characteristics (bubble size, bubble quantity, and mass transfer coefficient) of several different spargers. These characteristics include the rising velocity of bubbles and the contact time of the reactor system to increase dissolved oxygen (DO). Moreover, the consistencies of bubbles at different column heights and in different water sources has never been studied to achieve optimum floc removal efficiency; this research provides information on the optimal type of sparger for doing so to treat raw water.

A comparison of sparger capacities to produce microbubbles with different characteristics is needed to decide the microbubble generation method most economical and feasible for WTPs. The novelty of this study are (1) to investigate variations in bubble size to obtain the bubble rising velocity and (2) analyze microbubble mass transfer coefficient to determine the contact time needed to transfer DO into the liquid. These parameters are lack discussed and very significant because the sizes of bubbles and mass transfer coefficient are related in physical-chemical treatment for colloidal removal and contaminant oxidation.

2. Material and methods

2.1. Microbubble reactor setup

The microbubble reactor system has three tanks (see Figure 1). The first tank is the influent entry tank where the microbubbles are generated. The first tank is 90 cm high to allow flotation. The second tank is a connector tank with a height of 20 cm, and the third tank is a recirculation tank with a height of 20 cm.

Three local spargers were simulated for treating raw water into clean water. The first type was a vortex sparger that could be repositioned (unfixed) and was connected to a hose, inserted through the tank's top surface, and placed at the bottom of the tank. The second type was a venturi sparger placed in the same position as the vortex sparger (hereafter the “upper venturi”). The third sparger was also venturi and was placed at the bottom of the tank in a fixed position (hereafter the “lower venturi”). Figure 2 shows the schematic design of the three spargers.

2.2. Experimental stage

Prior to the actual experiment, a preliminary experiment was conducted to establish baseline bubble sizes using tap water (clean water) to produce the smallest bubble size for each sparger, as the smaller microbubbles more effectively capture floc and transfer mass into bulk solutions [8]. Three water flowrates were arranged using the valve and were read using a flowmeter. Each opening valve was combined with a different air flowrate. The water flowrates were set at 1.5 L/min, 1.0 L/min, 0.5 L/min, and 0.1 L/min because flowrates above 1.5 L/min produce milibubbles [2, 19]. Each combination of water flowrate and air flowrate was observed visually, and one of each had its corresponding microbubble picture taken. The pictures were analyzed using the software ImageJ to obtain the bubble sizes.

2.2.1. Viscosity measurement

During the actual experiment, river water was used as sample water to determine the abilities of the three spargers in the cases of actual polluted water. One hundred L of river water was sampled using a submerged pump in the center of a river cross-section. The dynamic viscosity of the sampled water in each sparger experiment was measured using an Ostwald Viscometer [20]. The calculation of dynamic viscosity was done by comparing the viscosity of the test results with the viscosity of distilled water, which has a dynamic viscosity at 29.6 °C (0.008038 Poise), as shown in Eq. (1):

$$\frac{\eta^{o}}{\eta} = \frac{\rho^{o} \cdot t^{o}}{\rho \cdot t} \tag{1}$$

where η^o is the viscosity of distilled liquid water, η is the viscosity of the sample liquid (Poise), ρ^o is the density of the distilled water (gr/mL), ρ is the density of the sample liquid (gr/mL), t^o is the time of the distilled water flow (sec), and t is the time of the sample liquid flow (sec).

2.2.2. Mass transfer coefficient calculation

During the actual experiment, DO concentrations were measured using an automated DO meter (Hanna HI98193) at a depth of 20 cm below the surface of the water, which allowed recording changes of DO concentration every minute. The mass transfer coefficients of the kLa fluid were obtained experimentally by plotting saturated DO concentrations every minute (CS-C) over time on semilog paper, where the slope produces kLa [8].

$$C = C_S - (C_S - C_0)e^{K_L at} \tag{2}$$

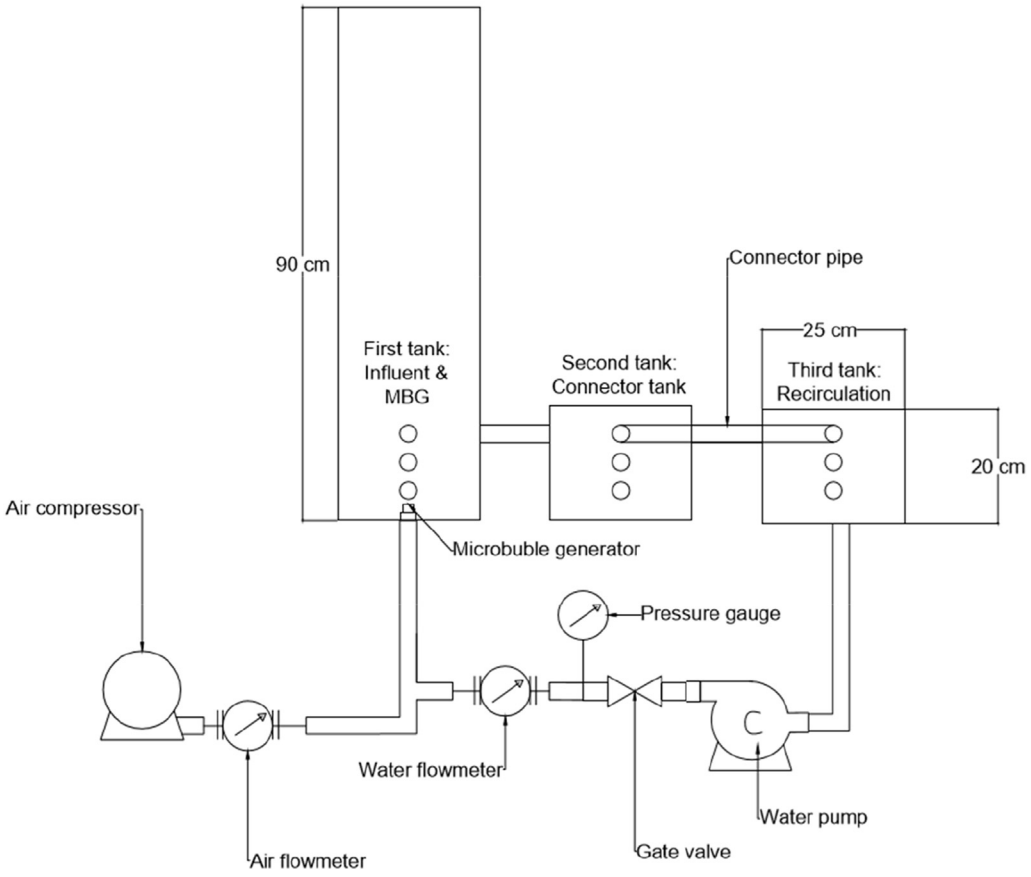

Figure 1. Configuration of the microbubble reactor system.

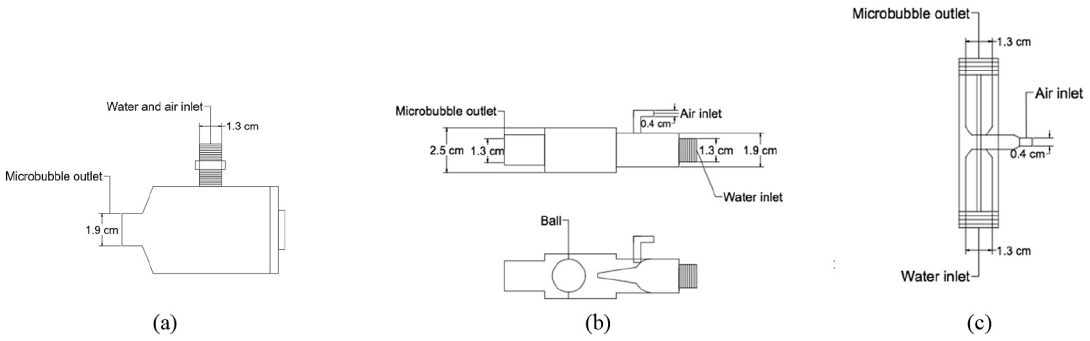

Figure 2. The three spargers: (a) vortex; (b) upper venture; and (c) lower venturi.

where *Cs* is the saturated DO concentration, C_0 is the initial DO concentration, and *C* is the desired DO concentration. After the slope value is obtained, the value is divided by the value of the *ln* to *log* constant (= 2.3). The kLa value obtained is in min^{-1} units, and all DO concentrations are in mg/L units. From Eq. (2), the contact time needed to increase DO concentration and the sparger's mass transfer coefficient can both be determined.

To maintain the kLa value, bubble size, and floatability, the law of similitude is used for scale-up to the actual case. When the volume is scaled up, the water flowrate can also be scaled up using Eq. (3):

$$Q = n^{2.5} q \tag{3}$$

where *n* is the scale-up volume multiplication, *Q* is the new flowrate of the sparger scale-up (L/min), and *q* is the initial flowrate of the sparger (L/min) [21].

2.2.3. Microbubble size measurement

The shooting of the microbubbles produced by each sparger was carried out using parallel, wide-view cameras arranged vertically to captures microbubbles at different heights, as Figure 3 shows.

A series of microbubble images were analyzed using ImageJ software [22] to measure the diameters and number of bubbles. The Feret diameter (the farthest distance between any two points in a restricted area) of each bubble, commonly used to measure diameters in 2D images [23, 24], represented each height. By Eq. (4), the mean diameter of each bubble was obtained from its Feret diameter [25].

$$D\,[1.0] = \frac{\sum_1^n D}{n} \tag{4}$$

where *D* is the mean diameter and *n* is the number of bubbles. With bubble diameter data, bubble rising velocity can theoretically be

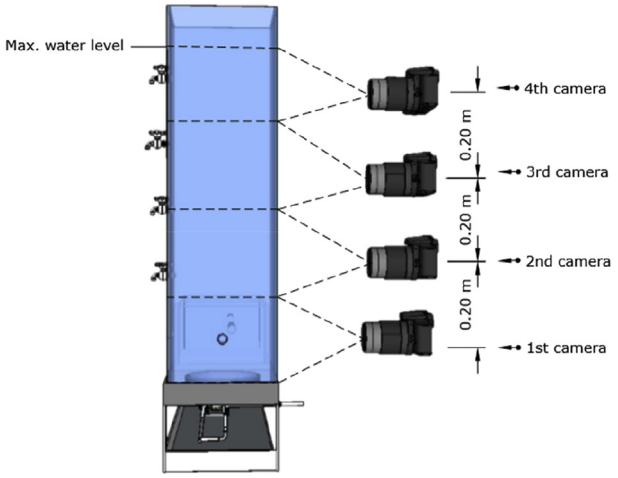

Figure 3. Schematic design of microbubble capture.

calculated using the mean bubble diameter and the dynamic viscosity of the sample water, the same process as calculating the force of gravity on laminar flow using Stokes's law [26, 27]. The bubble reaches an equilibrium between the force of gravity and the drag force when it reaches its terminal speed, as given by Eq. (5):

$$U = \frac{\rho g d^2}{18\mu} \tag{5}$$

where U is rising velocity (m/h), g is gravity acceleration (9.8 cm/s^2), d is the bubble diameter (cm), μ is the liquid dynamic viscosity (g/cm), and ρ is the liquid density (g/cm^3). The rising velocity affects the flotation unit retention time. The saturated retention time, τ (mins), is obtained from the water level height (h) divided by the rising bubble velocity ($\tau = h/U$). Retention time indicates how long the bubble lasts in the water [12].

The number of bubbles in the tank was calculated by employing the air flowrate, as the following equation shows:

$$N = \frac{\textit{air volume in the tank}}{\textit{individual bubble volume}} = \left(\frac{Q_a}{V_b}\right)\frac{h}{U} \tag{6}$$

where Q_a is the air flowrate (L/min), h is the sparger depth (m), U is the rising bubble velocity (m/h), and V_b is the volume of air bubbles on the liquid surface ($V_b = \frac{1}{6}\pi d^3$). The number of bubbles in the contact zone can be calculated using the following equation:

$$n = \frac{N}{Q_{L,in}\tau} \tag{7}$$

3. Results

3.1. Distribution of microbubble size for each sparger

In the preliminary experiment, each sparger produced microbubbles with various water flowrates and air flowrates. The vortex sparger with nozzle size 1.9 cm yielded variations in water flowrate of 3, 6, and 9 L/min at pressures of 0.6, 1.7, and 2.4 bar, respectively. The upper venturi sparger with nozzle size 1.3 cm yielded 6, 12, and 18 L/min at pressures of 0.5, 0.7, and 1.2 bar, respectively. The lower venturi sparger with nozzle size 1.3 cm yielded 6, 9, and 12 L/min at pressures of 0.4, 0.8, and 1.6 bar, respectively. With each variation of water flowrate and air flowrate, each sparger produced different microbubble sizes that were observed visually. Figure 4 presents the distribution of microbubble sizes.

The vortex sparger produced more opaque water than the other two spargers (at the largest water flowrate of 9 L/min, it produced microbubbles with air flowrates of 0.1, 0.5 and 1.0 L/min). With the lower venturi sparger, the water appeared more opaque at the highest water flowrate of 12 L/min with air flowrates of 0.1 and 0.5 L/min. The upper venturi sparger, in contrast, did not produce significant opacity, but the mean bubble size decreased as the water flowrate increased and the air flowrate decreased. The results of the bubble measurements in Table 1 show that the appearance of increasingly milky water correlated with smaller bubble sizes. The average vortex bubble size had the smallest value of 97 μm and the highest opacity. It has been demonstrated that the smallest air flowrate produces the smallest bubble size, so the water flowrates in the experiment were 9 L/min, 18 L/min, and 12 L/min for the vortex, upper venturi, and lower venturi spargers, respectively, with an air flowrate of 0.1 L/min for all the spargers.

3.2. Distribution of microbubbles at different heights

Capturing pictures using four cameras at different heights produced a microbubble size distribution. Bubble images were analyzed using ImageJ software and Feret diameters were obtained. Table 2 shows the average bubble size of each sparger from the lowest to the highest water

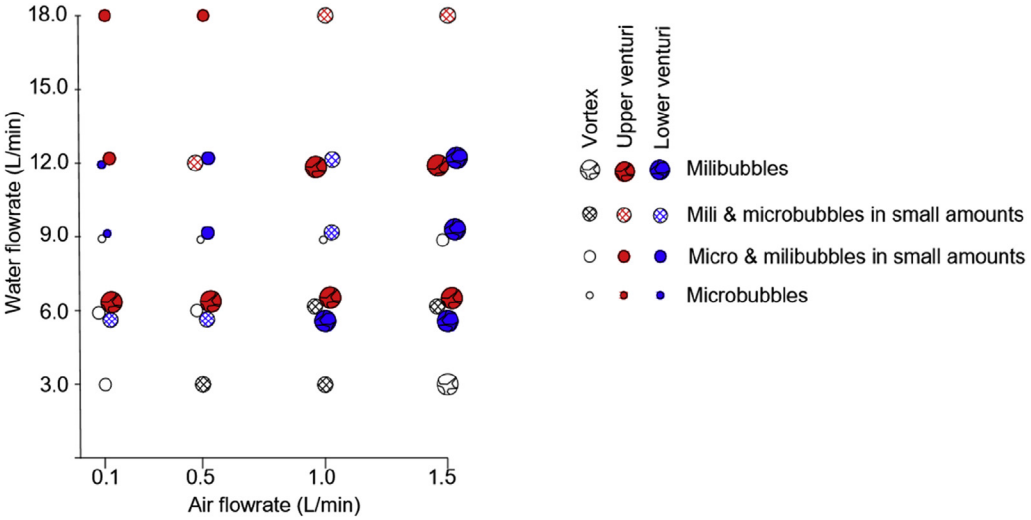

Figure 4. Distribution of microbubble sizes by sparger.

Table 1. Bubble diameters in preliminary experiment for the highest water flowrate with various air flowrates.

Mean bubble diameter (μm)				
Sparger type	air flowrate			
	1.5 L/min	1.0 L/min	0.5 L/min	0.1 L/min
Vortex	125	121	99	97
Upper venturi	145	119	115	107
Lower venturi	132	120	116	114

Table 2. Results of bubble diameters by sparger.

Sparger type	Bubble diameter	Camera 1 20 cm height (bottom)	Camera 2 40 cm height	Camera 3 60 cm height	Camera 4 80 cm height (top)	Overall tank mean diameter (*μm*)
Vortex	Mean (*μm*)	88	92	91	90	90
	Smallest bubble (*μm*)	49	49	46	49	
Upper Venturi	Mean (*μm*)	91	94	95	104	96
	Smallest bubble (*μm*)	51	45	49	48	
Lower Venturi	Mean (*μm*)	103	130	116	190	135
	Smallest bubble (*μm*)	50	52	53	55	

level, the smallest diameter at each height, and the mean diameter of the overall tank. The mean bubble diameters from camera 1 to camera 4 were obtained by Eq. (4), and the outlier data was crunched using a box and whisker plot. The trend was that, the higher the water level, the larger the average microbubble size. Of the three spargers, the vortex had the smallest average diameter of 90 μm, which was followed by the upper venturi with 96 μm and the lower venturi with 135 μm. The smallest bubble sizes at each height were not significantly different.

The dynamic viscosity measurements were 0.008373 g/cm.s, 0.008227 g/cm.s, and 0.008337 g/cm.s for the vortex, upper venturi, and lower venturi spargers, respectively. By employing these dynamic viscosities, the rising bubble velocity calculated using Stoke's Law (Equation 5) for the vortex, upper venturi, and lower venturi spargers were 17.67 m/h, 20.92 m/h, and 39.03 m/h, respectively (Figure 5). The number of bubbles that remains inside the tank all the time, was 735,833,907, 273,533,469, and 102,086,384 bubbles for the vortex, upper venturi, and lower venture spargers, respectively. The saturated retention times for the vortex, upper venture, and lower venturi were 2.7 minutes, 2.2 minutes, and 1.2 minutes, respectively.

3.3. Mass transfer coefficients caused by DO concentration changes

For the aeration process, the kLa value was obtained from the measurement of DO concentration. In experiments with the vortex sparger, the initial DO concentration was 1.92 mg/L. However, in 10 minutes, the DO concentration reached a stable condition of 6.45 mg/L (Figure 6). In the case of the upper venturi, the initial DO concentration was 1.69 mg/L and reached stable concentration at 5.56 mg/L in 17 minutes. For the lower venturi, the initial DO concentration was 2.28 mg/L and reached stability at 5.85 mg/L in 18 minutes.

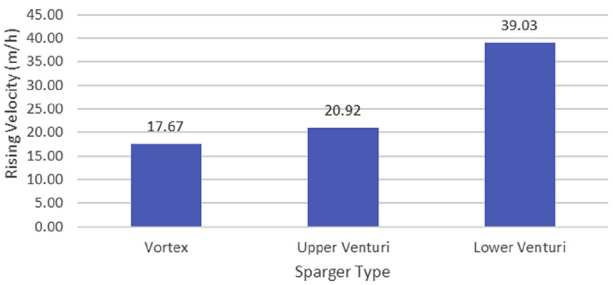

Figure 5. Rising velocities by sparger.

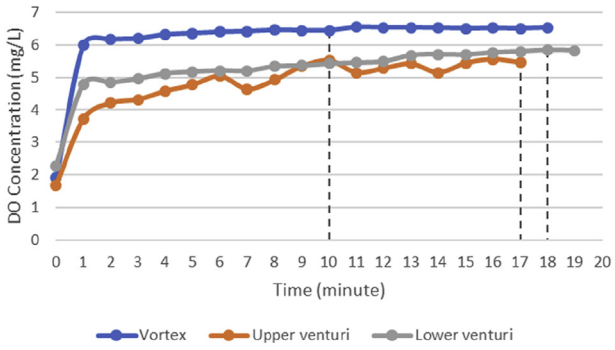

Figure 6. DO concentration changes vs. time.

The difference between saturated (stable) DO concentrations versus concentrations per minute was plotted on semilog graph paper (Figure 7a–c). The slope generated from the DO semilog graph versus time was converted using Eq. (2) to obtain the kLa value [8]. Of the three spargers, the vortex had the highest kLa value of 0.297/min, followed by upper venturi with 0.169/min and lower venturi with 0.183/min (Table 3).

kLa has an impact on the contact time required by one sparger to increase DO concentrations in certain liquids [28]. The simulation showed that increasing the DO concentration from an initial value of 1.5 mg/L to 6 mg/L took 3.64 minutes (vortex), 5.5 minutes (upper venture), and 5.92 minutes (lower venture). Assuming a scale-up of volume in the field up to twice that of the influent, the vortex sparger is obviously preferable, as it required the least water flowrate, that is, only 51 L/min.

4. Discussion

4.1. Sparger characteristics

The simulation results showed that, the greater water flowrate, the greater the water pressure shown by the pressure gauge. This phenomenon is consistent with Henry's Law, which indicates that the increased pressure from the sparger allows greater dissolution of gases into the water. In other words, pressure is directly proportional to the resulting equilibrium value [27]. As long as the saturation pressure produced by the vortex sparger is smaller than its critical value, the greater the saturation pressure, the smaller the bubbles produced [2]. In this study, the vortex sparger had the lowest water flowrate but produced the highest

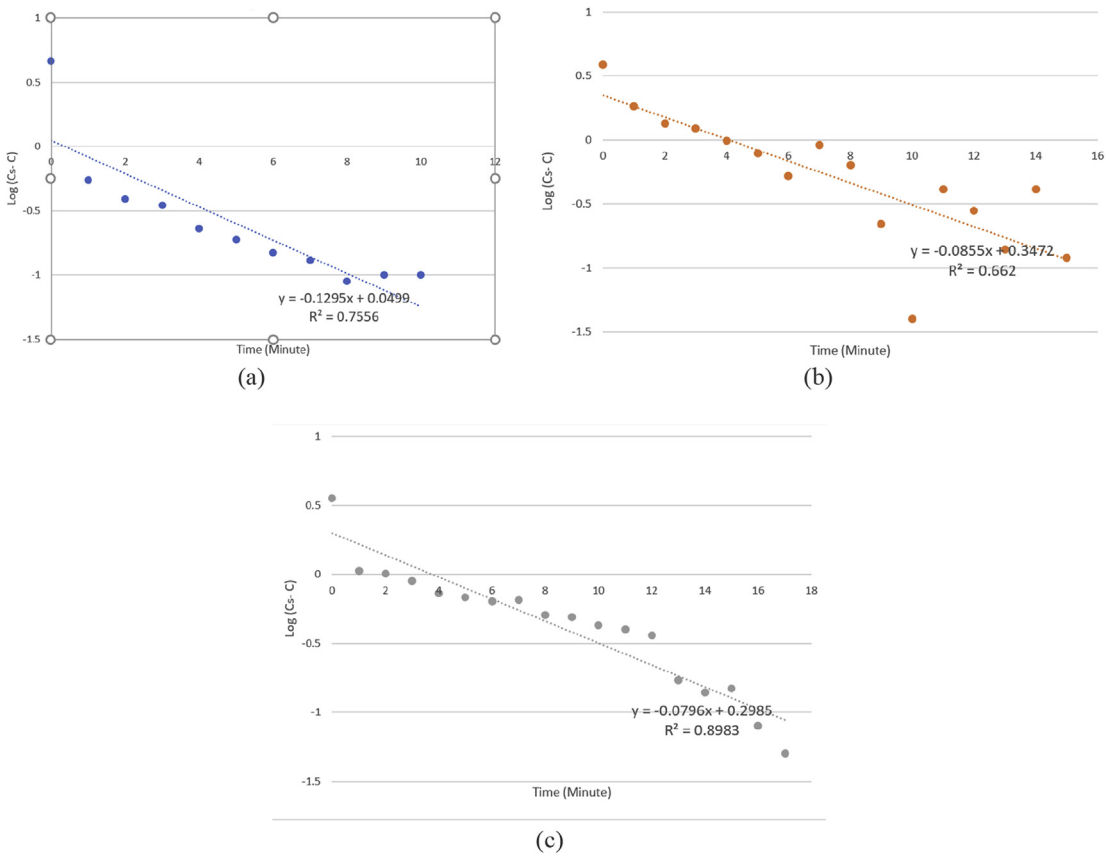

Figure 7. DO semilog plot by sparger: (a) vortex; (b) upper venture; and (c) lower venturi.

Table 3. Results of k_La contact time and scale-up water flowrate.

Type of sparger	kLa value (/min)	Contact time to reach 6 mg/L from initial concentration of 1.5 mg/L (min)	Water flowrate if the volume scaled-up twice (L/min)
Vortex	0.297	3.64	51
Upper venturi	0.169	5.50	102
Lower venturi	0.183	5.92	68

water pressure measured on the pressure gauge. In contrast, even though the lower venturi sparger had the highest water flowrate, it could not produce as much pressure as the vortex.

In Figure 4, the vortex sparger shows that, the smaller the air flowrate that is regulated and the greater the difference in the water flowrate, the smaller the bubbles and the whiter or "milkier" the water. The increasingly milky quality of the water indicates the presence of microbubbles in large quantities [29]. Thus, the vortex sparger combines the largest water flowrate and the smallest air flowrate in producing microbubbles.

Similar behavior occurs in the upper venturi and lower venturi spargers when the water flowrate increases and air flowrate decreases: The milibubbles reduce in size and microbubbles appear. Previous research [2] supports this finding, namely, that the greater the air flowrate, the more visible the bubbles are, and microbubbles are pegged at an air flow of around 0.5 L/min.

Of the three spargers, the smallest bubbles were generated by the highest water flowrate and the lowest air flowrate (vortex sparger). Li (2006) found that a maximum water/air ratio of 1:10 was obtained by the pressurization pump. In his study, the water/air ratios in the vortex sparger, upper venturi, and lower venturi were 1:80; 1:180, and 1:120, respectively. Thus, to ensure operational conditions favorable to the production of microbubbles, the water flowrates should be maximal, that is, approximately 9 L/min (vortex), 18 L/min (upper venturi), and 12 L/min (lower venturi).

A smaller air flowrate and greater pump pressure produces smaller bubbles [2, 19]. The importance of small bubble size is that it influences the bubble rising velocity and the bubble interfacial area, which, in turn, affects mass transfer and floc capture. In our study, the smallest bubble diameter was produced by the vortex sparger with an average air flowrate of 0.1 L/min: 99 μm. The sizes of the bubbles produced by the three spargers shrank because of the maximum gas dissolution of each sparger. Because the vortex used a pump while the venturi mixed the two phases (air and water) in the neck, the vortex managed to break the bubbles into smaller sizes [30]. The size of the bubbles resulting from depressurization is directly proportional to the flow pressure, the water flowrate, the air flowrate, and the pressure reduction mechanism [31] also the nozzle size. Small nozzle size might potentially increase the clogging. The venturi spargers have smaller nozzle size than vortex and perform more perishable. Besides, the air dissolved water might create membrane in the sparger as well that can increase clogging [32].

Though economically, the addition of sparger to generate microbubble will take an additional cost of the water treatment plant compared to conventional bubble technology. Besides the design of sparger, MBG needs a pump and air pressure to produce the microbubbles. Those additional instruments cost higher than a conventional bubble distributor that used only air compressor [12]. For example, a rough estimation of the relative cost required to scaled-up the air sparging devices and its tank in a treatment plant is around IDR 22 million (US$ 1,535). This cost

is based on the calculation of research results by extending to a scale up by a factor of 2 (estimation, taking into account the hydraulic load variation) with considering full scale capacity having sparger process efficiency about 75%. However, the level of technology and sparger types which efficient in removing pollutant and effective-cost can be selected carefully. Moreover, considering the ability of MBG to produce free radicals, microbubbles hold great potential for large scale application in treatment of water and waste effluent, and hence, should be a strong focus of research and process development [33].

4.2. Relation between bubble diameter and bubble rising velocity

As seen in Table 3, the higher the water level (up to camera 4), the bigger the microbubble diameter is. According to Laplace's equation, the size of the bubble is related to the pressure inside it or the pressure difference with its environment. Small bubbles have higher internal pressures than external [34]. Bubble formation begins with a horizontal surface shape. The radius of curvature then reduces to form a circle. In this phase, the bubble can be said to be in a stable condition. This condition is valid if the bubbles do not form hemisphere shapes [34]. No two bubbles, however, form the same way and so are not evenly sized. Some bubbles are large from the beginning, reducing pressure within the bubble. This allows gas to enter from outside again and reduce the pressure difference. Thus, such bubbles continue to grow and consequently become unstable [34].

As Table 2 shows, small bubbles were obviously still present at all heights (captured by cameras 2, 3, and 4) because small bubbles can maintain their perfectly spherical shapes [27] while larger bubbles transform into horizontal hemispheres. The flat hemisphere shape influences the buoyancy of the bubbles, forcing their paths to deviate as they rise to the surface [27]. This condition is unstable because the bubbles quiver when rising.

In the flotation process, the crucial balance is that the combined density of the particles and bubbles must be smaller than the density of water to float to the surface. Compared to other technology, microbubble generator (MBG) have been proved in enhancing the water treatment efficiency. It is because the use of MBG in the airlift pump system will increase the airlift performance, and so increasing the capability of the airlift pump for pumping flocs or sediments to the surface [35]. The main factor that influences the bubble rising velocity is bubble size. A smaller bubble will produce a slower rising velocity than a large one, which only produced by a microbubble generator instead of the conventional bubble generator. A slower rising velocity forces longer residence time, which creates contact time between particles and bubbles and consequently benefits flotation performance [27]. With microbubble's slower residence time, it benefits to collide and adhere more to particles that helps sediment removal through floating more efficient. The vortex sparger exhibited this effect with smaller bubbles resulting in a slower mean rising velocity of 17.67 m/h, which was followed by the upper venturi at 20.92 m/h and the lower venturi at 39.03 m/h.

Besides, based on Dobby and Finch model (1987), as particle diameter decreases, collision efficiency increases and attachment efficiency decreases that lead to induction time decreases [36]. Thus, this fact could be recovered by a smaller size bubble that has longer residence time to attach and entrap particle especially with intermediate to large size particle to float up to the water surface. Meanwhile, the collection efficiency for small particles is insensitive toward induction time [36].

Besides bubble size, the bubble rising velocity also depends on the temperature, the level of contamination, and the pressure on the system (as well as gravity, buoyancy, and drag force), whereas the viscosity has no significant effect [30]. As discussed earlier, along with increasing bubble size, there is a reduction in friction in the interfacial layer, which causes a faster rising velocity that impacts the retention time of the flotation unit. The retention time of the bubbles in the tank column with the water level at 80 cm was 2.7 minutes with the vortex sparger, 2.2 minutes with the upper venturi, and 1.23 minutes with the lower venturi. The vortex sparger had a bubble retention time close to the dissolved air flotation unit in general, that is, 2–3 minutes [31].

4.3. Mass transfer coefficient changes with contact time

Referring to Figure 6, we found that the vortex sparger experienced an increase in DO concentration of 4.63 mg/L, the upper venturi an increase of 3.87 mg/L, and the lower venturi an increase of 3.57 mg/L. The DO concentration was analyzed by involving the kLa calculation results. Next, a plotting log (C_s-C) took the gradient value to be converted into a mass transfer coefficient and plotted it versus time. Logs (C_s-C) are taken to a saturated point and not resumed to avoid both undersaturated and oversaturated conditions, as Henry's Law, that is, that the increased pressure from the sparger allows greater dissolution of gases into the water, only occurs in the chemical reaction between liquid and gas under equilibrium (saturated).

In Figures 7a, 7b, and 7c, the DO concentration associated with each sparger rises. The higher the kLa value, the faster the mass transfer rate. The vortex sparger produced the largest kLa of 0.297/min with a mass transfer rate of 1.37 mg/L.min, while the upper venturi and lower venturi produced 0.085/min and 0.079/min for kLa and 0.76 mg/L.min and 0.65 mg/L.min for the mass transfer rate, respectively. The main factors that influenced the increasing DO produced by each sparger were the sizes and shapes of the bubbles produced: Smaller bubbles have larger interfacial layer surface areas, thereby increasing gas hold-up. Gas hold-up functions as a concentration of the volume of bubbles that push the liquid out so that more gas occupies space [37]. This larger surface area also accelerates the gas exchange process into the solution. While oxygen increases in the solution, it helps to reduce the Biochemical Oxygen Demand (BOD) and Chemical Oxygen Demand (COD) that enhance the quality of water.

Also, bubble size affects the rising velocity, which, in turn, affects the mass transfer coefficient. As the bubbles grow, cell circulation or air movement inside the bubbles raises their velocities and reduce the friction at the interface that affects the kLa value. The long residence time driven by a slow rising velocity dissolves more oxygen in the liquid [38]. The shapes of the bubbles themselves also affect kLa: When they have shapes that are not perfect spheres or when they have increasingly distorted shapes due to their increasing size, they take irregular paths that are not straight to the water surface [27]. Moreover, large bubbles have a spiral track that can interfere and cause fusion with other bubbles [27].

The river water sample which had contaminants also affected kLa. Contaminants can be surfactants, which change the thicknesses of bubble cells and can reduce mass transfer [4]. Surfactants can also change the solubility of the incoming air and can form new interface layers that reduce the value of kLa. Surfactants can also accumulate thickness in the interface layer, which is an obstacle to gas diffusion and thereby further reduces the kLa value [27]. The last factor that influences the kLa value is mixing intensity: the more intense the mixing, the higher the kLa produced. A high mixing intensity increases the frequency of gas exchange and reduces the thickness of the interfacial layer, which increases the driving force of the solution to continue to absorb gas [27].

Referring to Table 3, large kLa values result in shorter contact times because the mass transfer capacity with a large kLa transfers oxygen faster so that an increase in DO concentration is easier to achieve fast dissolution the oxygen gas into water [12]. This condition only can be achieved by a micro-size bubble that is produced by MBG instead of conventional technology. The required water flowrate is also directly proportional to its original condition (before being scaled up); at the beginning, the upper venturi needed a higher water flowrate as the quantity of sample water increased. This factor, in fact, can be used as a consideration and measure of energy efficiency in the selection of a sparger. The vortex sparger had the lowest flowrate scale-up result of 51 L/min, the fastest contact time, and the best bubble size.

5. Conclusion

The most significant factor of microbubble technology effectiveness is bubble size. Smaller bubbles prove to perform better in microbubble generators in capturing floc and transfer gas. The vortex sparger reflected this fact, producing the smallest bubbles (mean diameter of 90 μm) and of the most bubbles in all the experimental trials. Smaller bubbles reduce bubble rising velocity, consequently giving bubbles more time to capture floc. On the other hand, the number of bubbles also plays an important role: Essentially, the number of bubbles must exceed the amount of floc to float. The smaller the bubbles, the greater the number of them that need to be generated. Again, the vortex sparger reflected this by producing the smallest bubbles and the most bubbles; it also had the shortest contact time of all the spargers (3.64 min). This shortest contact time gave the mass transfer coefficient (kLa) the highest value of 0.29/min. The larger the kLa value, the shorter the contact time in oxygen transfer into the solution (DO), which benefits the WTP process.

In sum, the results of this study contribute important data as the basis for developing efficient microbubble technology in terms of flotation an aeration processes for WTPs in Indonesia and other developing countries. Future Indonesian WTP development should consider using vortex spargers in the treatment of raw water to distribute to users, as this experiment has demonstrated their greater efficiency beyond any reasonable doubt. While expensive, it is only a matter of time before such spargers pay for themselves in cost savings. Future research can develop the technical operation condition for different raw water such as coagulant needs and the possibility of improving the bubble size itself.

Declarations

Author contribution statement

Nyoman Suwartha: Conceived and designed the experiments; Analyzed and interpreted the data; Wrote the paper.

Destrianti Syamzida: Conceived and designed the experiments; Performed the experiments; Analyzed and interpreted the data; Wrote the paper.

Cindy Rianti Priadi, Setyo Moersidik & Firdaus Ali: Contributed reagents, materials, analysis tools or data; Wrote the paper.

Funding statement

This study was financially supported by the Directorate Research and Community Engagement (DRPM) Universitas Indonesia under QQ Grants Scheme Number NKB-0317/UN2.R3.1/HKP.05.00/2019.

Competing interest statement

The authors declare no conflict of interest.

Additional information

No additional information is available for this paper.

Acknowledgements

The authors would like to thank the IWI for providing the laboratory and facilities for the experiment.

References

[1] D. Widhana, Suramnya Mutu Air Sungai Indonesia., Tirto.Id, tirto.id: https://tirto.id/suramnya-mutu-air-sungai-indonesia-cmnr, 2017. (Accessed 20 August 2011).

[2] P. Li, Development of Advanced Water Treatment Technology Using Microbubbles, PhD Diss, Keio Univ., Japan, 2006.

[3] K.K. Jyoti, A.B. Pandit, Water disinfection by acoustic and hydrodynamic cavitation, Biochem. Eng. J. (2001).

[4] S. Khuntia, S.K. Majumder, P. Ghosh, Microbubble-aided water and wastewater purification: a review, Rev. Chem. Eng. 28 (2012) 191–221.

[5] Y. Liu, Y. Zhou, T. Wang, J. Pan, B. Zhou, T. Muhammad, C. Zhou, Y. Li, Micro-nano bubble water oxygation: synergistically improving irrigation water use efficiency, crop yield and quality, J. Clean. Prod. 222 (2019) 835–843.

[6] Z. Li, Y. Zhang, Y. Han, K. Xie, Y. Fan, W. Shi, Water treatment experimental researches for microbubble flotation, coagulation deposition and microbubble coagulation floatation, in: Int. Conf. Chem. Civ. Environ. Eng., Istanbul, 2015, pp. 5–7.

[7] J. Wang, D. Li, Enhancing advanced oxidation process by microbubbles technology and the analysis of its degradation process, IOP Conf. Ser. Earth Environ. Sci. 146 (2018), 0–9.

[8] R. Droste, R. Gehr, Theory and Practice of Water and Wastewater Treatment, second ed., John Wiley & Sons, Inc., New Jersey, 2019.

[9] J. Gao, C. Li, P. Zhao, H. Zhang, G. Mao, Y. Wang, Insights into water-energy cobenefits and trade-offs in water resource management, J. Clean. Prod. 213 (2019) 1188–1203.

[10] C. Oliveira, R.T. Rodrigues, J. Rubio, A new technique for characterizing aerated flocs in a flocculation- microbubble flotation system, Int. J. Miner. Process. 96 (2010) 36–44.

[11] Q. Xu, M. Nakajima, S. Ichikawa, N. Nakamura, P. Roy, H. Okadome, T. Shiina, Effects of surfactant and electrolyte concentrations on bubble formation and stabilization, J. Colloid Interface Sci. 332 (2009) 208–214.

[12] K. Terasaka, A. Hirabayashi, T. Nishino, S. Fujioka, D. Kobayashi, Development of microbubble aerator for waste water treatment using aerobic activated sludge, Chem. Eng. Sci. 66 (2011) 3172–3179.

[13] T. Temesgen, T.T. Bui, M. Han, T. il Kim, H. Park, Micro and nanobubble technologies as a new horizon for water-treatment techniques: a review, Adv. Colloid Interface Sci. 246 (2017) 40–51.

[14] Wiratni Deendarlianto, A.E. Tontowi Indarto, A.G.W. Iriawan, The implementation of a developed microbubble generator on the aerobic wastewater treatment, Int. J. Technol. 6 (2015) 924–930.

[15] A.I. Majid, D. Aan, W. Wiratni, I. Indarto, Development of an Industrial-Scale Microbubble Generator for the Purposes of Aerobic Wastewater Treatment, 2016.

[16] Y. Van Fan, P.S. Varbanov, J.J. Klemeš, A. Nemet, Process efficiency optimisation and integration for cleaner production, J. Clean. Prod. 174 (2018) 177–183.

[17] A. Azevedo, R. Etchepare, J. Rubio, Raw water clarification by flotation with microbubbles and nanobubbles generated with a multiphase pump, Water Sci. Technol. 75 (2017) 2342–2349.

[18] F. Ali, D.L. Lestari, M.D. Putri, M. Yehuda, The Effectiveness of Microbubble for the Quality Improvement of Water Bodies, 2017, pp. 3–6.

[19] S.Y. Jeon, J.Y. Yoon, C.M. Jang, Bubble size and bubble concentration of a microbubble pump with respect to operating conditions, Energies 11 (2018) 1–13.

[20] M. Ujvári, Determination of viscosity with Ostwald viscometer, Fiz. Kémiai Tanszék (2014). https://phys.chem.elte.hu/turi/SysPhysChem/Materials/Viscosity_Ostwald.pdf.

[21] G. de Thierry, Application of the law of similitude to hydraulic laboratory research, Proc. Natl. Acad. Sci. Unit. States Am. 13 (1927) 684–688.

[22] J. Fiabane, P. Prentice, K. Pancholi, High yielding microbubble production method, BioMed Res. Int. 2016 (2016).

[23] ImageJ, Menu Commands. https://imagej.nih.gov/ij/docs/guide/146-Part-V.html, 2012. (Accessed 21 April 2019).

[24] O. Hernandez, F. Ndoye, H. Benkhelifa, D. Flick, G. Alvarez, A discriminating microscopy technique for the measurement of ice crystals and air bubbles size distribution in sorbets, Refrig. Sci. Technol. (2015) 2564–2571.

[25] D.J. Wesley, D.T.W. Toolan, S.A. Brittle, J.R. Howse, W.B. Zimmerman, Development of an optical microscopy system for automated bubble cloud analysis: publisher's note, Appl. Optic. 55 (2016) 7392.

[26] M.A.R. Talaia, Terminal velocity of a bubble rise in a liquid column, Eng. Technol. 22 (2007) 264–268.

[27] M. Benjamin, D. Lawler, Water Quality Engineering: Physical/Chemical Treatment Processes, John Wiley & Sons, Inc., New Jersey, 2013.

[28] K. Yao, Y. Chi, F. Wang, J. Yan, M. Ni, K. Cen, The effect of microbubbles on gas-liquid mass transfer coefficient and degradation rate of COD in wastewater treatment, Water Sci. Technol. 73 (2016) 1969–1977.

[29] A. Agarwal, W.J. Ng, Y. Liu, Principle and applications of microbubble and nanobubble technology for water treatment, Chemosphere 84 (2011) 1175–1180.

[30] A.A. Kulkarni, J.B. Joshi, Bubble formation and bubble rise velocity in gas-liquid systems: a review, Ind. Eng. Chem. Res. 44 (2005) 5873–5931.

[31] L. Wang, N. Shammas, W. Selke, D. Aulenbach, Flotation Technology, Humana Press, New York, 2010.

[32] T. Hasegawa, A. Ushida, M. Goda, Y. Ono, Organic compounds generated after the flow of water through micro-orifices: were they synthesized? Heliyon 3 (2017).

[33] G. Kaushik, A. Chel, Microbubble technology: emerging field for water treatment, Bubble Sci. Eng. Technol. 5 (2014) 33–38.

[34] V. Tesař, Microbubble generation by Fluidics. Part II: bubble formation mechanicsm, Proc. Colloq. Fluid Dyn. Prague. 1 (2012) 1–20.

[35] I. Supraba Deendarlianto, A.I. Majid, M.R. Pradecta, A. Indarto, Widyaparaga, Experimental investigation on the flow behavior during the solid particles lifting in

a micro-bubble generator type airlift pump system, Case Stud. Therm. Eng. 13 (2019) 100386.
[36] S. Rao, Surface Chemistry of Froth Flotation, Second Edi, New York, 2004.
[37] A. Thriveni, B. Swathi, K. Sivadhanya, N. Murty, K. V Ramesh, Gas holdup in a gas-liquid upflow bubble column in the presence of doublecone promoter, ChemXpress 6 (2014) 108–115.
[38] W. Fan, Z. Zhou, W. Wang, M. Huo, L. Zhang, S. Zhu, W. Yang, X. Wang, Environmentally friendly approach for advanced treatment of municipal secondary effluent by integration of micro-nano bubbles and photocatalysis, J. Clean. Prod. 237 (2019) 1–8.